



Great Lakes Maritime Research Institute

*A University of Wisconsin - Superior and
University of Minnesota Duluth Consortium*

Further Development and Optimization of the Ballast-Free Ship Design Concept

Final Report

Michael G. Parsons Arthur F. Thurnau Professor Emeritus
Professor Emeritus of Naval Architecture and Marine Engineering
Phone: 734-945-2886; FAX: 734-936-882; e-mail: parsons@umich.edu

Miltiadis Kotinis Assistant Professor, Mechanical Engineering, Old Dominion University
Phone: 757-683-5939; FAX: 757-962-5097; e-mail: mkotinis@odu.edu

October 30, 2008

Department of Naval Architecture and Marine Engineering
University of Michigan
2600 Draper Road
Ann Arbor, MI 48109-2145



This report represents the results of research conducted by the authors and does not necessarily represent the views or policies of the Great Lakes Maritime Research Institute. This report does not contain a standard or specified technique. The authors and the Great Lakes Maritime Research Institute do not endorse products or manufacturers. Trade or manufacturers' names appear herein solely because they are considered essential to this report.

*Research funded in part by the Great Lakes Maritime Research Institute.
This study was supported by the U.S. Maritime Administration
Grant # DTMA1-G-06-005*

Table of Contents

	page
1. Introduction	1
2. Background	2
2.1 Development of the Seaway-sized Bulk Carrier	4
2.2 Arrangement and Design of Inlet and Outlet	6
3. Numerical Investigation	8
3.1 External Flow	8
3.2 Internal Flow	15
4. Experimental Investigation	16
5. Potential Economic Impacts of the Research Results	20
6. Dissemination of Study Results	22
7. References	25

List of Tables

	page
Table 2.1: Main Particulars of the Ballast-Free Bulk Carrier	5
Table 2.2: Characteristics of the Ballast-Free Bulk Carrier Model in Ballast Condition	5
Table 3.1: Grid Independence Study	10
Table 3.2: Drag Coefficients and Form Factor	10
Table 3.3: Nominal Axial Wake Fraction	14
Table 4.1: Form Factor Comparison	17
Table 4.2: Characteristics of the MHL No. 20 and No. 23 Propellers	17
Table 4.3: Propulsion Test Results – Ballast Condition at 15.5 Knots	18

List of Figures

	page
Figure 2.1: Schematic of the Ballast-Free Ship Concept	2
Figure 2.2: Typical Seaway-size Bulk Carrier (left); Ballast-Free Concept Bulk Carrier (right)	3
Figure 2.3: Bow View of the Seaway-sized Bulk Carrier Model	5
Figure 2.4: Stern View of the Seaway-sized Bulk Carrier Model	5
Figure 2.5: Location of Forward Ballast Trunk Inlet	6
Figure 2.6: Location of Two Ballast Trunk Discharges Investigated	7
Figure 3.1: Bow Grid Detail of the Ballast-Free Bulk Carrier in Ballast Condition	8
Figure 3.2: Stern Grid Detail of the Ballast-Free Bulk Carrier in Ballast Condition	8
Figure 3.3: Bow Pressure Coefficient Contours of the Ballast-Free Bulk Carrier (baseline no trunk flow case)	9
Figure 3.4: Stern Pressure Coefficient Contours of the Ballast-Free Bulk Carrier (baseline no flow case), Outlet Locations Shown for Reference	9
Figure 3.5: Stern Pressure Coefficient of the Ballast-Free Bulk Carrier (discharge Sta. 17 – 90 min)	11
Figure 3.6: Stern Pressure Coefficient of the Ballast-Free Bulk Carrier (discharge Sta. 19 – 90 min)	11
Figure 3.7: Stern Pressure Coefficient of the Ballast-Free Bulk Carrier (discharge Sta. 17 – 120 min)	11
Figure 3.8: Stern Pressure Coefficient of the Ballast-Free Bulk Carrier (discharge Sta. 19 – 60 min)	12
Figure 3.9: Axial Velocity Contours in the Propeller Plane (baseline no trunk flow case)	12
Figure 3.10: Axial Velocity Contours in the Propeller Plane (discharge Sta. 17 – 90 min)	13
Figure 3.11: Axial Velocity Contours in the Propeller Plane (discharge Sta. 19 – 90 min)	13
Figure 3.12: Axial Velocity Contours in the Propeller Plane (discharge Sta. 17 – 120 min)	14

Figure 3.13: Axial Velocity Contours in the Propeller Plane (discharge Sta. 19 – 60 min)	14
Figure 3.14: Computational Model of Double Bottom Ballast Trunk Structure	15
Figure 4.1: Ballast-Free Bulk Carrier Total Resistance	16
Figure 4.2: Ballast-Free Bulk Carrier Effective Power	17
Figure 4.3: Stock Propeller Open Water Characteristics and Ship Thrust Requirement	19
Figure 5.1: Order of Magnitude Economics Comparing a Typical Bulk Carrier with Filtration and UV Treatment with Ballast-Free Bulk Carrier	21

Executive Summary

The initial investigation of the Ballast-Free Ship concept demonstrated the feasibility of the concept through a thorough examination of various design aspects. The effectiveness of the concept, in terms of eliminating the transport of foreign ballast water from ships operating in the ballast condition, was also demonstrated by utilizing Computational Fluid Dynamics (CFD) software to simulate the flow in the double bottom ballast trunks of the vessel. Nevertheless, this initial investigation did not succeed in showing the full cost-effectiveness of the concept. The main reason was a significant fuel penalty that resulted from an increased power requirement found in the initial hydrodynamic testing of a non-optimized discharge configuration on an existing, higher-speed vessel with a non-optimum propeller.

The ongoing GLMRI sponsored research project has undertaken further hydrodynamic investigation of the Ballast-Free Ship concept; both experimental and numerical. The experimental investigation was performed by utilizing the Seaway-size bulk carrier model that was designed and built as part of the initial phase of this project. Resistance and propulsion tests were performed with this model in the towing tank of the University of Michigan Marine Hydrodynamic Laboratory in January 2007. The initial numerical investigations were performed utilizing the commercial CFD software FLUENT®.

The computational results were utilized both as guidance for the experimental setup and also to corroborate the experimental results. Specifically, the selection of the trunk flow inlet and outlet locations utilized in the towing tank experiments was guided by the numerical results. The ballast trunk flow inlet was located in the center of the bulbous bow. Two different locations were tested for the water discharge: one at the level of the upper part of the propeller disk close to Station 17 (near the forward engine room bulkhead, full scale) and one lower close to Station 19 (near the aft engine room bulkhead).

The experiments in the towing tank consisted of detailed resistance and propulsion testing with and without the ballast trunk flow. The analysis of the model test data revealed that the experimental results were in good agreement with the numerical results. Overall, discharging water at the stern of the model slightly increases ship resistance, but proper design of the discharging arrangements can overcome this negative effect. Another source of modest ship resistance increase is the trunk inlet at the bow. Given the limited positive-pressure region at the bow of the full form bulk carrier under consideration, an inlet location other than that currently utilized will probably result in a significant reduction in the available pressure differential, without providing a noteworthy benefit in terms of ship resistance.

Nonetheless, the proper water discharge at the stern of the vessel can have a favorable effect on the propulsion characteristics for the Seaway-size bulk carrier design investigated. The reduction in powering requirements, relative to the initial unmodified design, at an assumed ballast speed of 15.5 knots was found in the January 2007 experiments to be 7.3% for water discharge close to Station 17 and 2.1% for water discharge close to Station 19. The gain in overall propulsive efficiency outweighs the increase in ship resistance. The large power decrease of 7.3% was, however, suspect leading to additional work during in the current year.

Additional numerical work was performed during the past year using the Star-CCM+[®] CFD software that includes the v^2 -f turbulence modeling that has been found to be more effective for fuller hull forms as in the Seaway-sized bulk carrier under consideration. Additional model-scale experiments were also undertaken in the towing tank of the University of Michigan Marine Hydrodynamic Laboratory in July 2008. These experiments utilized improved methods for the resistance testing and this provided more consistent results and higher total resistance increases with the use of the Ballast-Free trunk flow than found in the January 2007 experiments. With the discharge at Station 19, the resistance increase in the ballast condition at 15.5 knots was found to be 2.44% full scale. With the discharge at Station 17, the resistance increase at the ballast condition at 15.5 knots was found to be 4.61%.

When the required propulsion power was determined, it was found to decrease by 1.63% from the unmodified case with the preferred discharge at Station 17. This results from a change in the propeller operating point and changes in the flow over the stern due to the ballast trunk flow introduction into the boundary layer so that it increases the flow into the upper part of the propeller disk. This results in increases in the propeller operating efficiency and also the hull efficiency that are large enough to offset the increase in the total resistance measured without the propeller. These results confirm the required power decrease found in the January 2007 experiments, but show that those results were unrealistically high.

In order to investigate the economic benefit of the aforementioned propulsive improvements, an operating scenario for the grain trade to Europe was adopted for the Ballast-Free bulk carrier. The change in the Required Freight Rate (RFR) with respect to an alternative filtration and UV ballast treatment system was estimated. The net savings would be about \$1.00 per tonne of cargo for the Ballast-Free bulk carrier with the water discharged close to Station 17. The overall ship design would also benefit from placement of the water discharge near the forward engine room bulkhead. A different operating scenario could result in even lower savings. Nevertheless, cost-effectiveness combined with a numerically-demonstrated foreign-ballast-elimination capability confirms the Ballast-Free Ship concept will be a viable alternative to more costly ballast treatment systems. Even though the current project focuses on a smaller Seaway-size bulk carrier, the concept should also be applicable to other new-construction ships of different types and sizes.

1. Introduction

The Ballast-Free Ship Concept was invented (US Patent #6,694,908 2004) and initially investigated (Kotinis et al. 2004, Kotinis 2005, *Ballast Water News* 2004) at the University of Michigan as a way to minimize the risk of the further introduction of nonindigenous aquatic species into the Great Lakes and other coastal waters by ships arriving in the ballast condition. Even though the feasibility of the concept was demonstrated, the initial analysis was limited by its required comprehensive research scope and limited associated budget. Thus, it was only feasible to support model testing that utilized an existing model. Although the vessel type of greatest interest for the Great Lakes nonindigenous aquatic species introduction problem is the Seaway-sized bulk carrier, the best available model was of a relatively finer, higher-speed barge-carrying Lighter Aboard Ship (LASH) vessel. The results with this finer model indicated a significant 7.4% power penalty with the use of the Ballast-Free Ship concept.

The first year of GLMRI sponsored research (Parsons and Kotinis 2006) supported the design of a typical Seaway-sized bulk carrier and the construction of a scaled model to be utilized in subsequent towing tank experiments. This model was designed, constructed, and delivered in 2006. The goal was to use this model to optimize the location of the Ballast-Free trunk discharges in order to reduce or eliminate the propulsion power increase observed with the modified LASH model. Experimental and numerical hydrodynamic investigations, combined with an optimization procedure, were expected to lead to a design solution that could offer a net required power reduction and savings in Required Freight Rate (RFR) relative to alternate ballast water treatment methods and approaches.

In the second year of GLMRI sponsored research (Parsons and Kotinis 2007), the hydrodynamic aspects of the Ballast-Free Ship concept were further investigated both experimentally and numerically. Part of the numerical investigation, including discharge location design optimization, was reported in a paper presented at the 9th International Conference on Numerical Ship Hydrodynamics (Kotinis and Parsons 2007a). The experimental hydrodynamic investigation, supported by the Computational Fluid Dynamics (CFD) analysis and an economic analysis, was presented at the Annual Society of Naval Architects and Marine Engineers (SNAME) Meeting in November 2007 (Kotinis and Parsons 2007b). This work showed a significant 6.3% net required power reduction that needed further confirmation.

In the current year of GLMRI sponsored research, the hydrodynamic aspect of the Ballast-Free ship concept was further investigated both numerically and experimentally. The Ballast-Free bulk carrier model, utilized in prior phases of the investigation, was employed as the investigated model hull. The numerical part was performed using the Star-CCM+[®] commercial CFD software. Various aspects of the flow were examined; the appropriate locations for the inlet/outlet, the form factor as a function of flow rate, the nominal wake, and the internal trunk flow. The experimental investigation was performed in July 2008 in the Marine Hydrodynamics Laboratory (MHL) towing tank of the University of Michigan. The qualitative effect of the water suction and discharge on the resistance of the bulk carrier model was determined and the results were extrapolated to full scale. Furthermore, the effect on propulsion and the economics was also examined utilizing a second propeller of the same diameter as the one utilized in the previous year experiments (Kotinis and Parsons 2007b).

2. Background

The initial Sea Grant supported development of the Ballast-Free Ship Concept was reported in a paper before the Annual Meeting of the Society of Naval Architects and Marine Engineers (SNAME) in Washington, DC, in October 2004 (Kotinis et al. 2004). Overall, the investigation of the Ballast-Free Ship Concept has shown that it provides a viable alternative to the addition of costly ballast water treatment systems in order to meet the evolving performance requirements for ballast water treatment. The concept essentially eliminates the transport of foreign ballast water. This should be more effective than current treatment methods in reducing the potential for the further introduction of nonindigenous aquatic species into the Great Lakes and coastal waters. Furthermore, it should be equally effective as international requirements extend below the 50 micron range (IMO 2004).

The traditional approach to ballast operations, since the introduction of steam machinery, has been the use of water ballast to increase the weight of the vessel in the light cargo condition. A paradigm shift in thinking here views the ballast condition as a change of buoyancy rather than an addition of weight in order to get the vessel to its safe ballast drafts. Such a shift in thinking led to the invention of the Ballast-Free Ship Concept (US Patent #6,694,908 2004).

In this concept, the traditional ballast tanks are replaced by longitudinal, structural ballast trunks that extend beneath the cargo region of the ship below the ballast draft. A schematic of this concept is shown in Fig. 2.1.

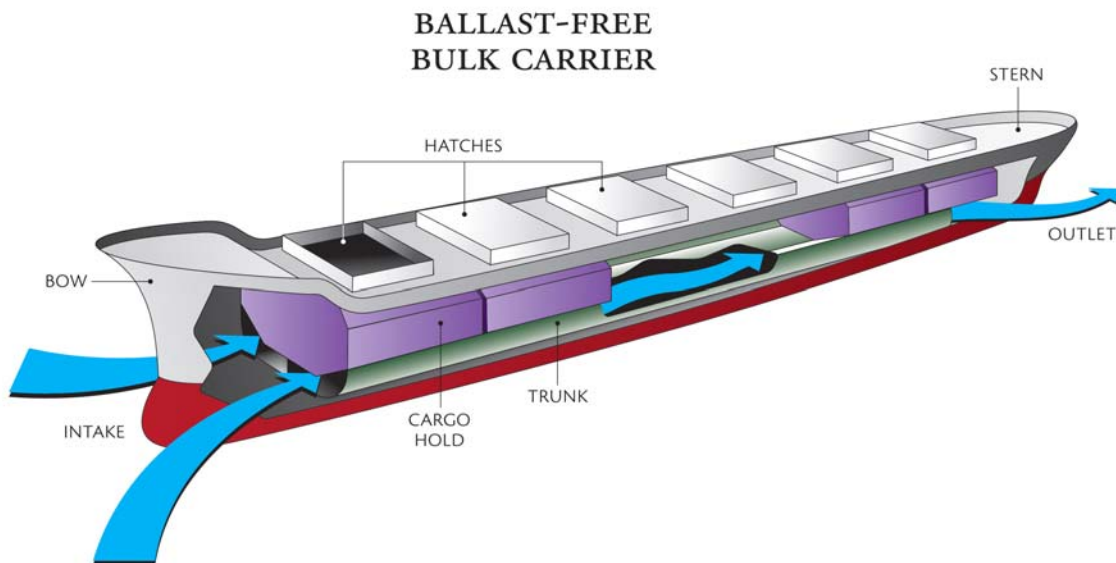


Figure 2.1: Schematic of the Ballast-Free Ship Concept

The arrangement of a conventional Seaway-size bulk carrier is shown on the left in Fig. 2.2; the arrangement of an equal grain capacity Ballast-Free Ship Concept Seaway-size bulk carrier is shown for comparison on the right. In this example, the three ballast trunks per side are connected to the sea through a plenum at the bow and a second plenum at the stern. These trunks

are flooded with seawater to reduce the buoyancy of the vessel in the ballast condition in order to get the vessel down to its ballast drafts. Since there is a natural hydrodynamic pressure differential created between the bow region and the stern region of a ship due to its motion through the water, a slow flow is induced in these open ballast trunks. This ensures that the ballast trunks are always filled with slowly-moving “local seawater.” This should ensure that there is no transport nonindigenous aquatic species across the globe. Therefore, the vessel becomes foreign “ballast-free” from the traditional viewpoint.

When the ballast voyage is completed, the ballast trunks can be isolated from the sea by valves and then pumped dry using conventional ballast pumps. The need for costly ballast water treatment equipment or ballast water treatment chemicals would, thus, be eliminated. This approach would also be equally effective for biota smaller than 50 microns. During the full load condition or any condition where ballast is not necessary, the outer four ballast trunks would be segregated utilizing valves at each of the cargo hold bulkheads. This is needed to provide the vessel adequate damage survivability under current IMO requirements.

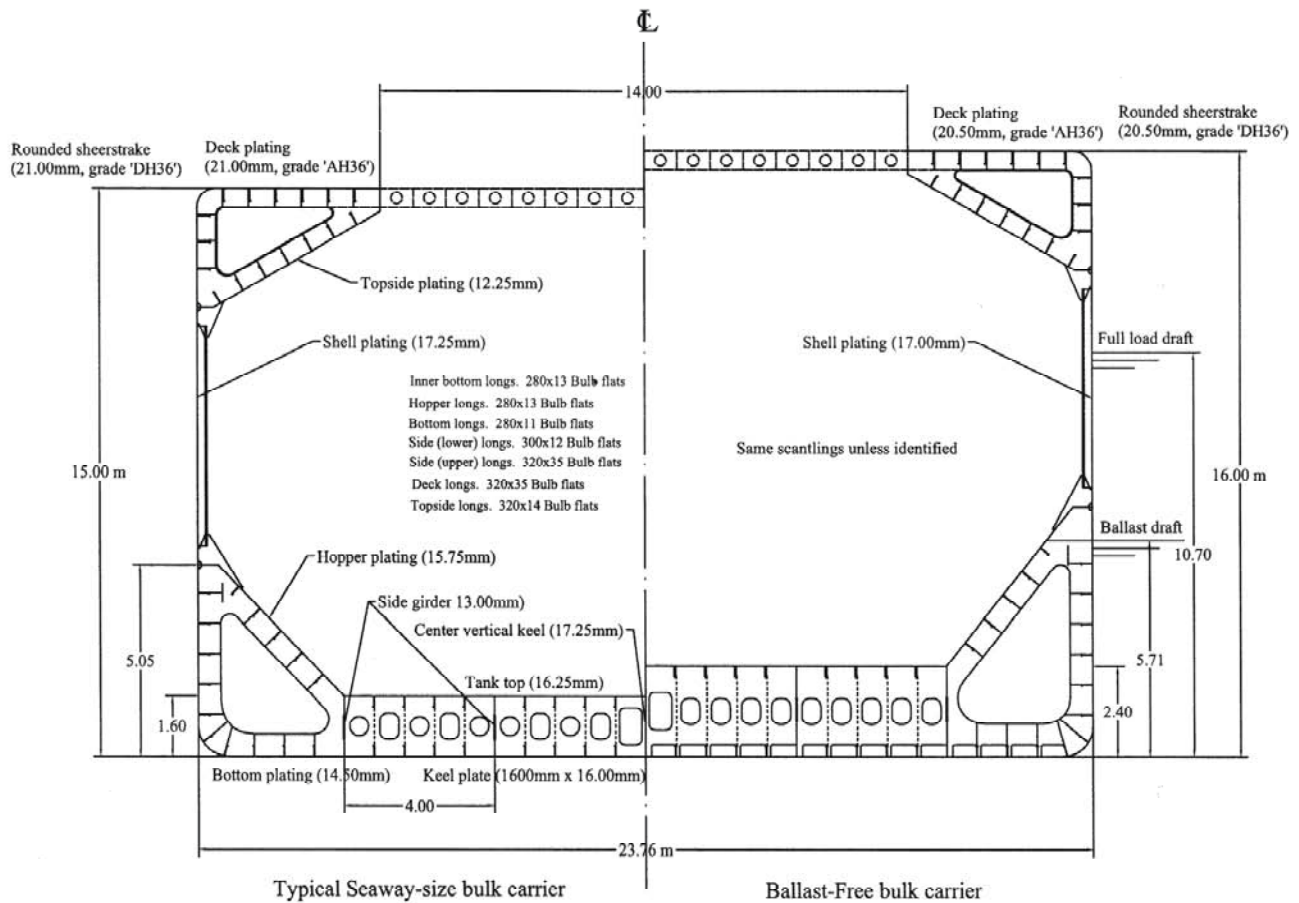


Figure 2.2: Typical Seaway-size Bulk Carrier (left); Ballast-Free Concept Bulk Carrier (right)

In order to provide adequate intact stability, equivalent damage survivability, equivalent cargo capacity, etc., the entire vessel design needs to be developed to support this concept of ballast operations as illustrated in Fig. 2.2. Thus, it is not feasible for back fit and is suitable only for new construction. The ship requires a higher tank top in order to locate enough ballast trunk

volume below the ballast draft and requires a greater hull depth in order to maintain the vessel's capacity to carry light cargos, such as grain. The Ballast-Free Ship Concept also includes features to minimize the buildup of sediment within the ballast trunks and facilitate their required cleaning; i.e., easier to clean 2.4 m high ballast trunks and the elimination of the lower part of the floors next to the shell.

As noted, the initial research on the development of the Ballast-Free Ship Concept was limited by its required comprehensive research scope and limited associated budget. For budgetary reasons, it was only feasible to support model testing that utilized an existing model. Although the vessel type of greatest interest for the Great Lakes nonindigenous aquatic species introduction problem is the Seaway-size bulk carrier, the best available model was of a relatively finer, higher-speed barge-carrying Lighter Aboard Ship (LASH) vessel. This existing model was modified to utilize a more conventional stern, but the model test results were not directly applicable to the Seaway-size bulk carriers studied in detail in the rest of the research effort.

The initial model tests had to be limited to a single system design for the existing model. There was no opportunity to optimize the hydrodynamic design of the system to minimize the economic impact of the Ballast-Free Ship Concept design. The initial model tests using the modified LASH vessel hull showed that the specific ballast intake and discharge locations and method tested resulted in a modest 2.2% increase in resistance, but a more significant 7.4% increase in the required propulsion power. This specific result assumed a change in the ballast water within the ballast trunks once every two hours, which would meet the environmental intent of the Ballast-Free Ship Concept. The large power increase could result in an undesirable engine size increase and would certainly result in an important fuel cost penalty. In that investigation, it was concluded that further hydrodynamic optimization could eliminate most, if not all, of this significant added power requirement.

This undesirable power penalty motivated the GLMRI sponsored research effort that has designed a Seaway-sized bulk carrier, produced a 5 m precision scale model of that vessel, undertaken Computational Fluid Dynamics (CFD) analyses of this design, and conducted hydrodynamic testing of the model in the University of Michigan Marine Hydrodynamics Laboratory (MHL). The primary goal of this research has been the optimization of the ballast trunk intake and discharge configurations in order to provide a required power reduction rather than an increase, if feasible.

2.1 Development of the Seaway-sized Bulk Carrier

The Ballast-Free bulk carrier model, which was designed and built during the initial GLMRI sponsored phase of this project (Parsons and Kotinis 2006), was tested at the University of Michigan Marine Hydrodynamics Laboratory (MHL) in January of 2007 in year two. The main particulars of the ship are shown in Table 2.1. The characteristics of the model in the ballast condition are presented in Table 2.2. The bow and the stern of the constructed model are shown in Figs. 2.3 and 2.4, respectively. All of the initial tests were carried out at the ballast drafts at which the Ballast-Free trunks would be in use.

Table 2.1: Main Particulars of the Ballast-Free Bulk Carrier

Waterline length (m)	195.5
Maximum beam (m)	23.76
Depth to main deck (m)	16.00
Full-load draft (m)	10.70
Block coefficient C_B	0.835

Table 2.2: Characteristics of the Ballast-Free Bulk Carrier Model in the Ballast Condition

Geometric scale ratio λ	37.92
Waterline length (m)	5.00
Maximum beam (m)	0.627
F.P. draft @ 40% DWL (m)	0.113
A.P. draft @ 70% DWL (m)	0.198
Wetted surface area (m ²)	5.34



Figure 2.3: Bow View of the Seaway-sized Bulk Carrier Model



Figure 2.4: Stern View of the Seaway-sized Bulk Carrier Model

2.2 Arrangement and Design of Ballast Trunk Inlet and Outlets

A full-scale diameter of approximately 1 m was chosen for the plena inlet and outlet to ensure a smooth inflow and outflow without imposing severe constraints on the structural arrangements. The corresponding inlet/outlet diameter at model scale is approximately 2.6 cm. The flow rate in the longitudinal trunks was calculated assuming a full-scale volume of ballast water equal to 18,500 m³. This value was obtained from similar ships, under the assumption of flooding both the normal ballast tanks and a central cargo hold for a heavy weather ballast condition. Assuming an exchange time of 90 min and utilizing Froude scaling, the internal flow rate at model scale is $Q_m = Q_s \lambda^{-5/2} = 3.9 \cdot 10^{-4} \text{ m}^3/\text{s}$. Using the continuity equation and assuming a symmetrical plenum about the centerplane, the average discharge fluid speed is 0.382 m/s.

The selection of the inlet location was based primarily on providing a pressure differential capable of sustaining a steady trunk (internal) flow. In addition to this, the inlet must be adequately submerged to avoid air ingestion and interaction with the free surface and the bow-generated wave system. An important design constraint is the low forward draft in the ballast condition. It was decided to locate the water inlet right on the face of the bulbous bow in the area around the stagnation point to take advantage of the high positive pressure in this region. Therefore, the center of the water inlet was placed at approximately 25% of the design waterline (DWL) above the keel as shown in Fig. 2.5.



Figure 2.5: Location of Forward Ballast Trunk Inlet

In order to investigate the effect of the water discharge on the flow at the stern, two different discharge locations were selected; one close to Station 17 and one close to Station 19 as shown in Fig. 2.6. Station 17 is approximately at the location of the forward engine room bulkhead in the full-scale ship; Station 19 is approximately at the aft engine room bulkhead. The discharge at Station 17 was located high at about the 45% DWL and the discharge at Station 19 was located lower at about the 30% DWL. The flow was discharged at about 10 degrees to the local hull surface. In this way, the effect on the boundary layer flow, as well as the effect on propeller inflow, could be investigated in a systematic manner.

The choice of the discharge locations investigated was based on the results of a numerical CFD investigation. These results are presented in the next section. If trunk flow rate maximization

were the only criterion, the water outlet should be located in an area with high suction pressure to maximize the pressure differential. On the other hand, when the propeller operation is taken into account, the real objective should be to minimize the ship's power requirement subject to achieving adequate ballast trunk flow.

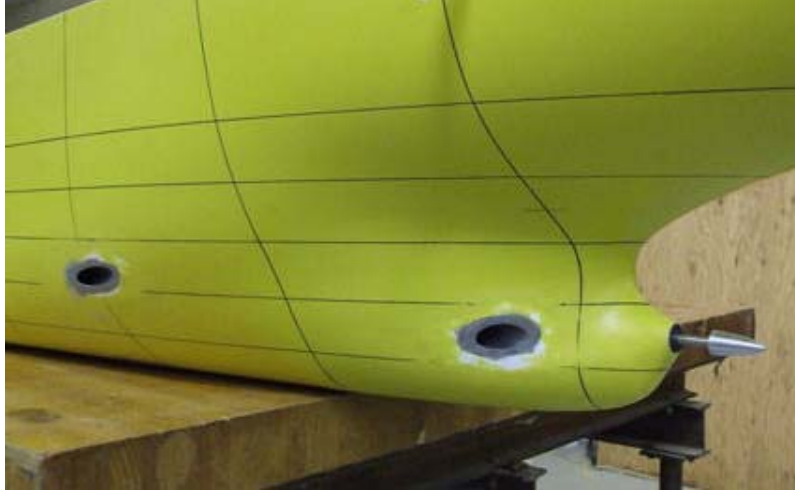


Figure 2.6: Location of Two Ballast Trunk Discharges Investigated

3. Numerical Investigation

3.1 External Flow

The numerical investigation of the flow around the Ballast-Free Concept bulk carrier model was performed using the Star-CCM+[®] CFD software during the recent year. A predominantly hexahedral grid, details of which are shown in Figs. 3.1 and 3.2, was utilized. Star-CCM+[®] was used instead of FLUENT[®], as used in the previous work, because the turbulence could be simulated using the v^2 -f turbulence model, which has been more successful in predicting the wake characteristics of full hull shapes. The boundary layer flow was resolved all the way to the solid boundary (hull), as one of the goals was the successful prediction of the mixing between the boundary layer flow and the water discharge at the stern. The v^2 -f turbulence model is theoretically valid throughout the flow domain without the need for turbulence damping functions in the viscous sublayer. Therefore, the mesh was created to provide the required refinement close to the hull.

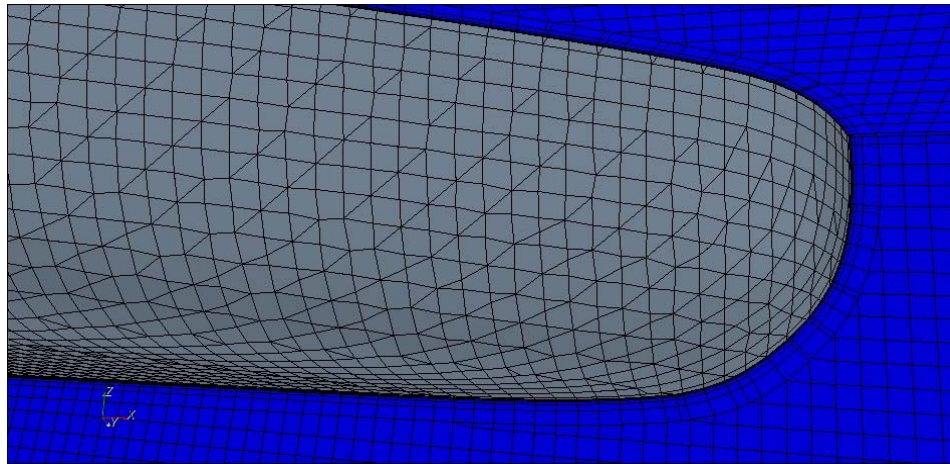


Figure 3.1: Bow Grid Detail of the Ballast-Free Bulk Carrier in Ballast Condition

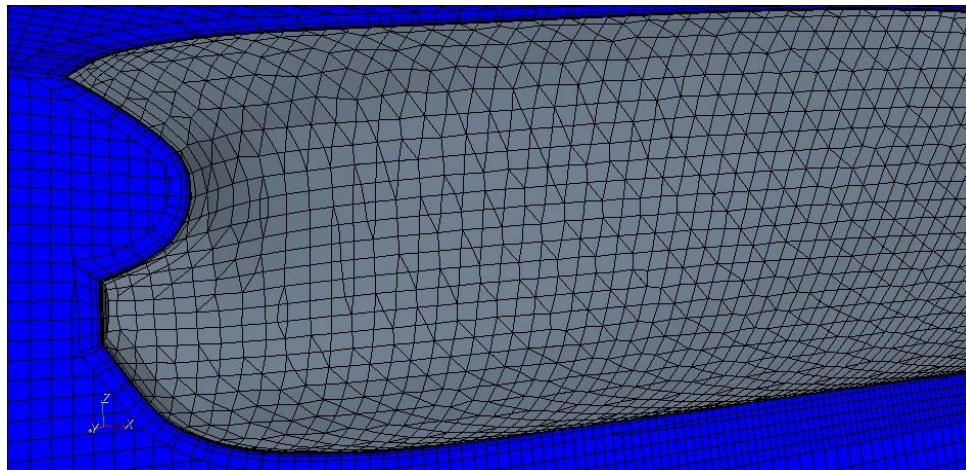


Figure 3.2: Stern Grid Detail of the Ballast-Free Bulk Carrier in Ballast Condition

The positioning of the water inlet at the bow of the Ballast-Free bulk carrier was established using the earlier CFD results. A plot of the Star-CCM+[®] pressure coefficient distribution, at the ballast drafts and speed, is shown in Fig.3.3. The magenta is the highest pressure, while the blue-greens and blues represent a negative pressure. The high block coefficient of this hull form limits the region of positive pressure at the bow and, consequently, the alternatives for the bow inlet position. It was decided to place the inlet right on the tip of the bulb to ensure that there would be an adequate pressure differential to drive the trunk flow. This configuration was utilized in both sets of towing tank testing (January 2007 and July 2008) as well as in the numerical hydrodynamic investigations.

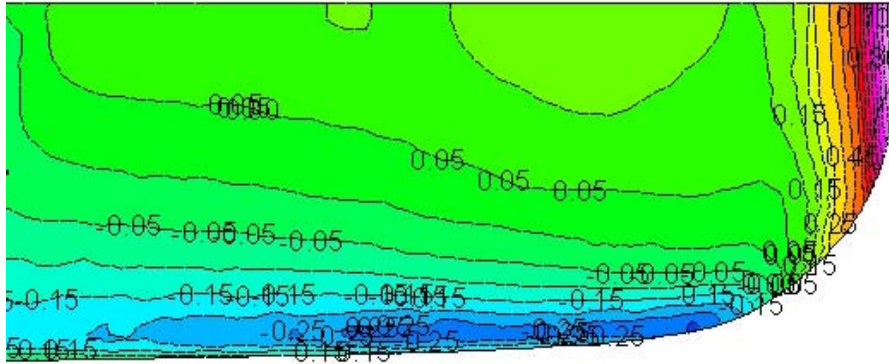


Figure 3.3: Bow Pressure Coefficient Contours of the Ballast-Free Bulk Carrier (baseline no trunk flow case)

Two discharge locations at the stern of the vessel were tested as shown on the model. These two locations are shown in Fig. 3.4 together with the pressure coefficient contours at the stern of the Ballast-Free bulk carrier while in ballast draft and speed, but with no trunk flow. There is a relatively flat suction pressure region near Station 17, which could provide a steadier internal (trunk) flow. As noted, the selected discharge location in this region offers an additional benefit as it would be close to the forward engine room bulkhead, thus, obviating the need for extending the trunks through the engine room. During the experimental investigation in January 2007, both these discharge locations provided a reduction in the propulsive requirements, leading to savings in the Required Freight Rate (RFR). The better Station 17 location was further investigated in 2008 to confirm the very large required power improvement (-7.3%) found in the 2007 tests.

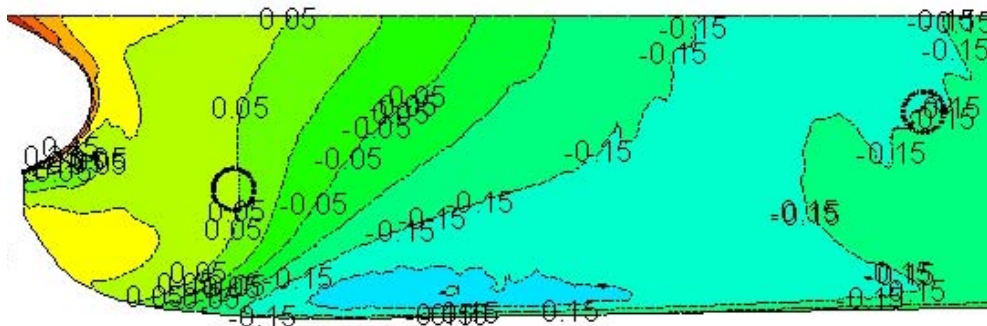


Figure 3.4: Stern Pressure coefficient Contours of the Ballast-Free Bulk Carrier (baseline no flow case), Outlet Locations Shown for Reference

Prior to deriving conclusions based on the numerical results, a grid convergence study was carried out in order to obtain a grid-independent solution. The investigation was performed in model scale (geometric scale factor of 37.92) in order to be able to perform direct comparisons with the experimental results. The grid convergence was evaluated by comparing the pressure, friction, and total drag coefficients of systematically refined grids. Given the unstructured nature of the generated grids, a systematic refinement was performed mainly in the area close to the hull (and within the boundary layer) setting a goal for an approximate grid refinement ratio of $\sqrt{2}$.

The ballast speed in full scale was assumed to be 15.5 knots. The computational model did not include a free surface; therefore, the results do not include wave drag and can be utilized directly for the form factor calculation. An additional assumption pertains to the trunk flow speed. This was computed utilizing an exchange time for the ballast water of 90 min, which is equivalent to a model scale flow rate of 6.1 gpm, assuming that the flow is scaled to maintain Froude number similarity, in a manner similar to the external flow scaling.

The model-scale simulations were run on a PC equipped with a quad-core 2.66 MHz processor and 8 GB of RAM running in 64-bit Windows Vista. A full-scale simulation of the flow has not been successful thus far, as the near-wall meshing requirements to allow for the flow mixing cannot be handled appropriately by the currently utilized grid generator.

As shown in Table 3.1, the solution in the fine grid can be considered grid-independent. Subsequently, this grid was utilized in all simulations. The results in Table 3.2 reveal that the pressure drag coefficient is lower when the internal flow is simulated. It can be postulated that the major contribution to the pressure coefficient reduction comes from the placement of the water suction at the tip of the bulbous bow, which causes a significant pressure relief in this region producing a form drag reduction. The pressure coefficient contours at the stern with discharge near Stations 17 and 19 are shown in Figs. 3.5 and 3.6, respectively.

Table 3.1: Grid Independence Study

Grid (# of cells)	Baseline case		
	C_P	C_F	C_T
Coarse (581,162)	0.960e-3	3.225e-3	4.185e-3
Medium (815,402)	0.937e-3	3.366e-3	4.303e-3
Fine (1,176,085)	0.936e-3	3.377e-3	4.313e-3

Table 3.2: Drag Coefficients and Form Factor

	C_P	C_F	C_T	Form Factor
Baseline no trunk flow case	0.936e-3	3.377e-3	4.313e-3	0.315
Discharge at St. 17 – 90min	0.906e-3	3.375e-3	4.281e-3	0.306
Discharge at St. 19 – 90min	0.921e-3	3.378e-3	4.299e-3	0.311

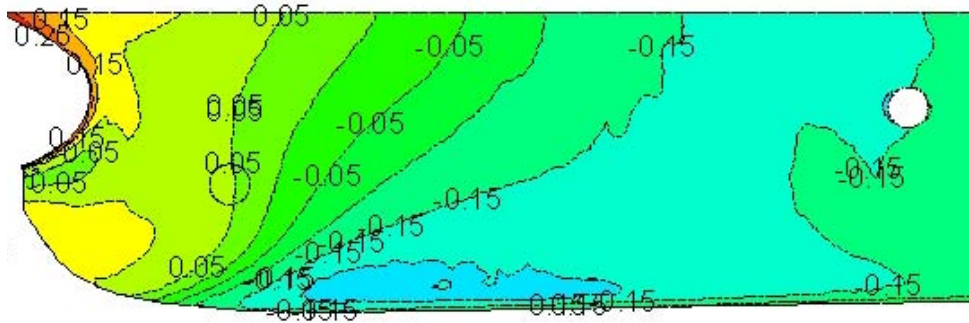


Figure 3.5: Stern Pressure Coefficient of the Ballast-Free Bulk Carrier (discharge Sta. 17 – 90 min)

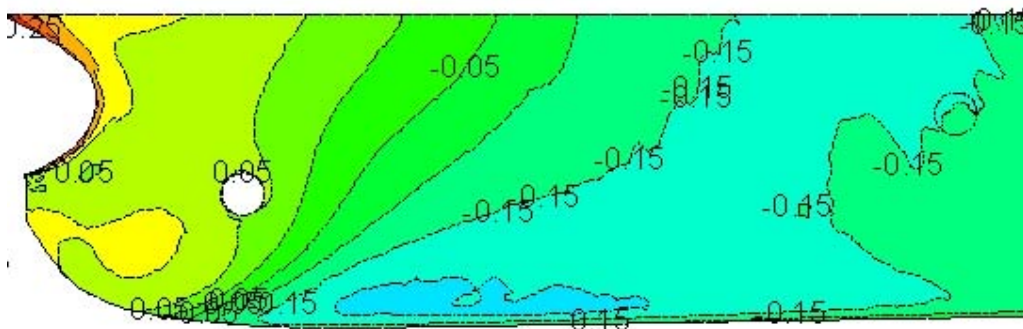


Figure 3.6: Stern Pressure Coefficient of the Ballast-Free Bulk Carrier (discharge Sta. 19 – 90 min)

Additional runs were performed to investigate the flow rate effect on the resistance. Specifically, runs were made for an exchange time of 120 min, and thus, a slower water discharge, and also an exchange time of 60 min leading to higher discharge velocities. The first, slower case was investigated using the discharge location near Station 17 as this is a relatively higher pressure region which is less likely to provide a high exchange rate. The computed pressure drag coefficient has a value of $0.884e-3$ and the friction drag coefficient has a value of $3.375e-3$. The computed pressure drag coefficient value corresponds to a substantial reduction compared to the 90-min water exchange case with discharge from the same location. The resulting form factor value is 0.299. The pressure coefficient contours at the stern of the vessel in this case are shown in Fig. 3.7.

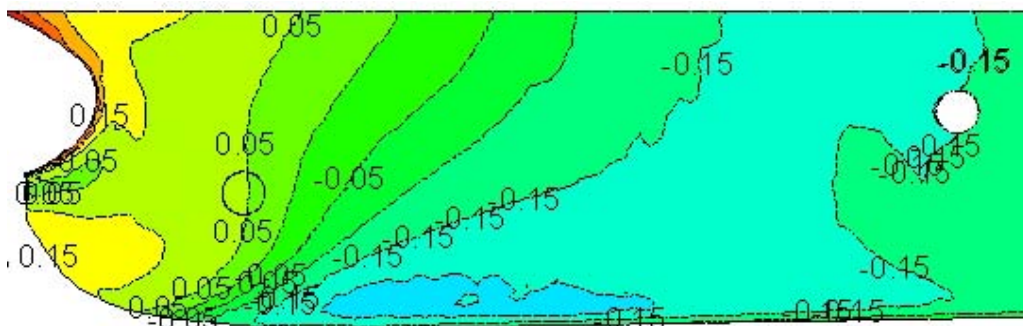


Figure 3.7: Stern Pressure Coefficient of the Ballast-Free Bulk Carrier (discharge Sta. 17 – 120 min)

The case with discharge near Station 19 was further investigated using a higher flow rate corresponding to a ballast exchange time of 60 min. The major consequence of the increased flow rate is a significantly higher pressure drag coefficient, which diminishes the benefits obtained through the bow water suction. The computed values of the pressure and friction drag coefficients are $0.932e-3$ and $3.379e-3$, respectively. The corresponding form factor value is 0.315. The pressure coefficient contours at the stern of the vessel in this case are shown in Fig. 3.8.

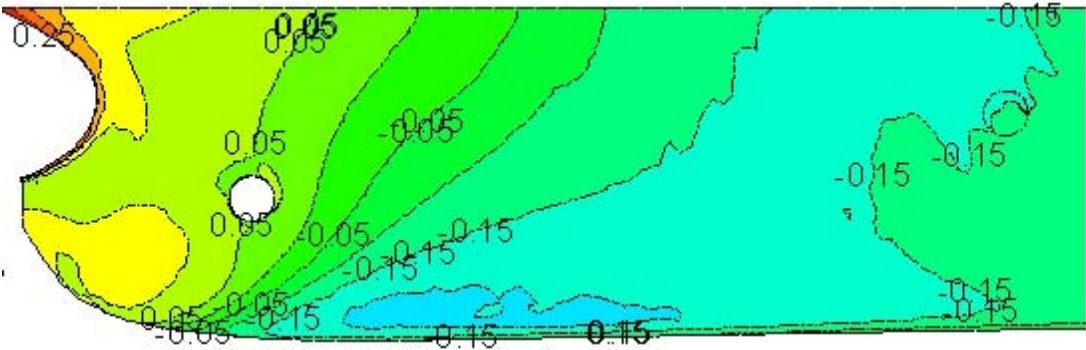


Figure 3.8: Stern Pressure Coefficient of the Ballast-Free Bulk Carrier (discharge Sta. 19 – 60 min)

The discharge effect on the nominal hull wake was studied by computing the nominal wake fraction. The corresponding values for each of the aforementioned cases are listed in Table 3.3. Plots of the axial velocity at the propeller plane are shown in Figs. 3.9 through 3.13. The results reveal that a faster discharge flow provides a more uniform wake, even though, as pointed out earlier, this leads to higher pressure drag. On the other hand, the discharge at Station 19 provides a more homogeneous, but slower, wake at lower radii.

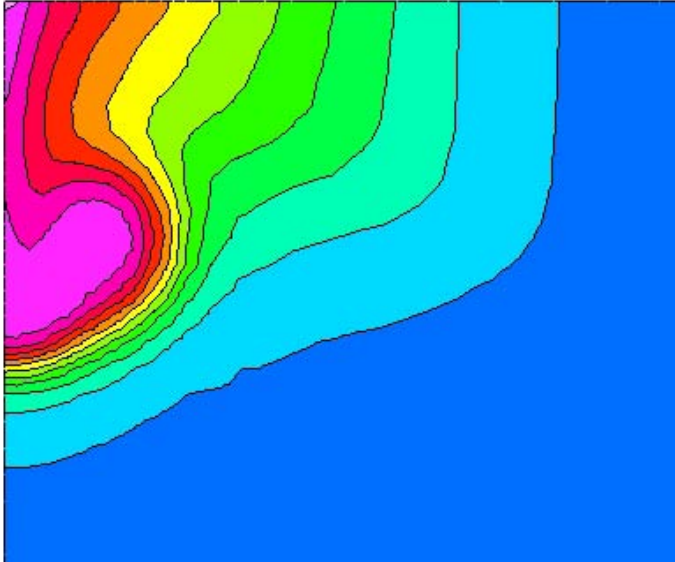


Figure 3.9: Axial Velocity Contours in the Propeller Plane (baseline no trunk flow case)

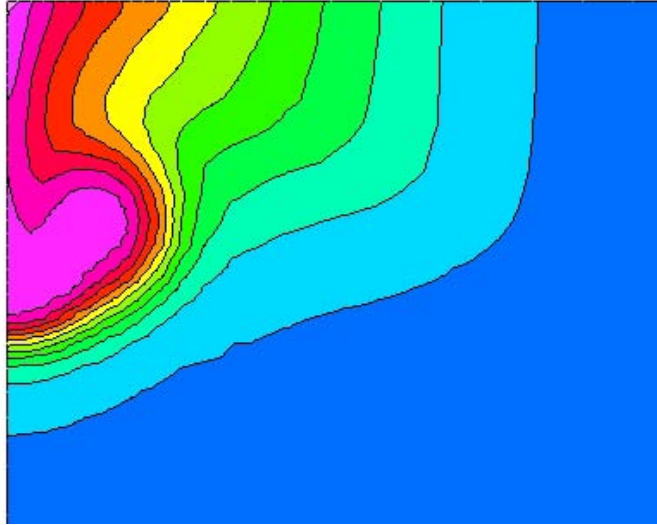


Figure 3.10: Axial Velocity Contours in the Propeller Plane (discharge Sta. 17 – 90 min)

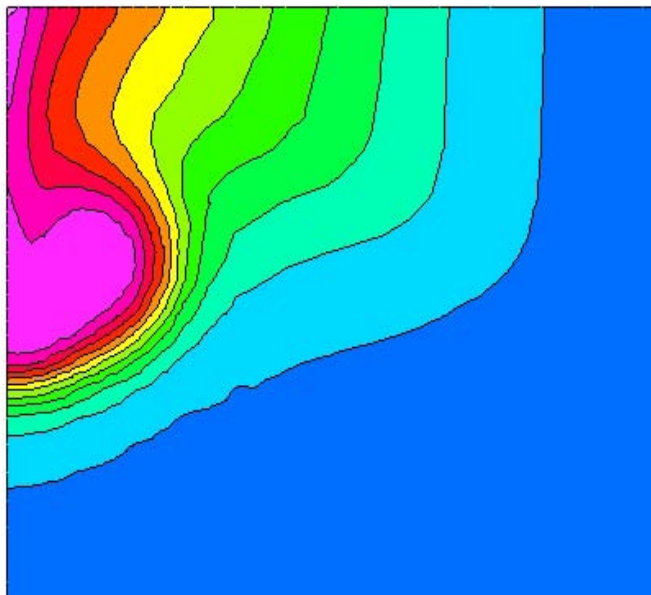


Figure 3.11: Axial Velocity Contours in the Propeller Plane (discharge Sta. 19 – 90 min)

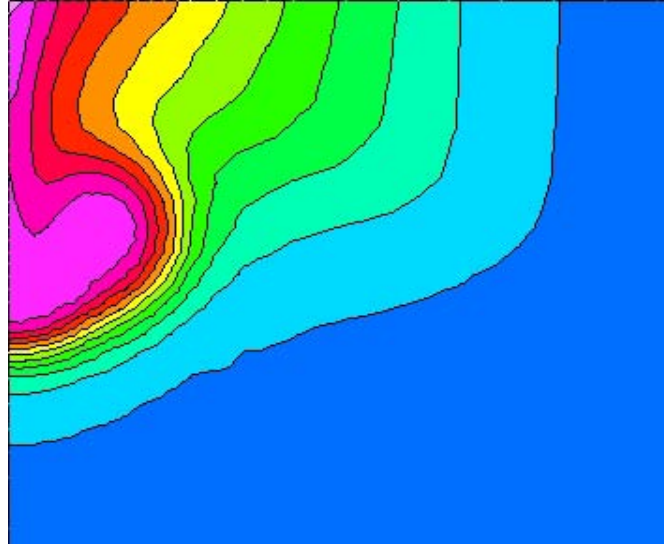


Figure 3.12: Axial Velocity Contours in the Propeller Plane (discharge Sta. 17 – 120 min)

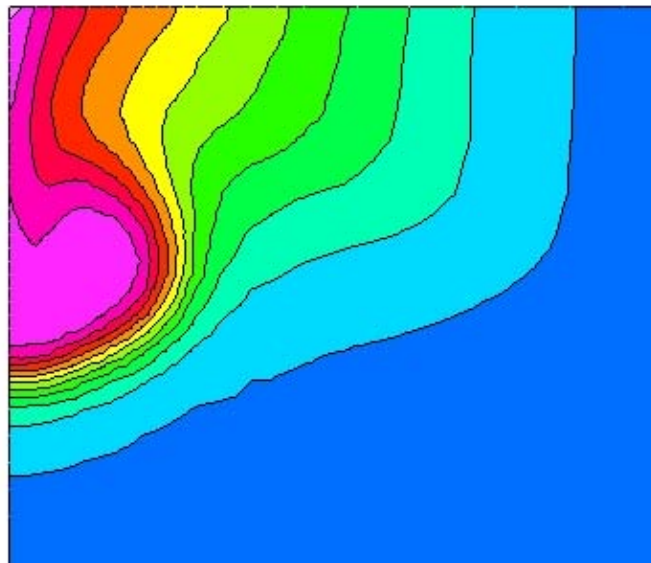


Figure 3.13: Axial Velocity Contours in the Propeller Plane (discharge Sta. 19 – 60 min)

Table 3.3: Nominal Axial Wake Fraction

	w_H
Baseline no trunk flow case	0.405
Discharge at St. 17 – 90min	0.402
Discharge at St. 19 – 90min	0.438
Discharge at St. 17 – 120min	0.408
Discharge at St. 19 – 60min	0.427

3.2 Internal Flow

The trunk flow was simulated by utilizing the computational model of the initial investigation of the Ballast-Free ship concept (Kotinis et al. 2004). The domain of the internal flow consists of the trunks in six cargo holds connected via sluice gates. The double bottom structures were modeled as accurately as possible, as shown in Fig. 14. Due to the center plane symmetry, only half of the domain was modeled. Even though the inlet location has changed since the initial investigation, it was decided to utilize the original configuration in order to compare the effect of the turbulence model on the calculations. The turbulence model utilized in this case was the v^2 -f model within Star-CCM+[®]. The objective was to compute the time required to flush the existing water inside the trunks. The pressure differential was set equal to 0.50. The concentration of the water that enters the trunks through the pressure inlet ('new water') was monitored and utilized as the stopping criterion. Specifically, three new water concentration levels for the entire array of ballast trunks were considered: 95%, 99%, and 99.9%. The respective recorded times were 85.0, 108.5, and 139.4 minutes. All these times are slightly lower than those obtained earlier using FLUENT[®] (Kotinis et al. 2004).

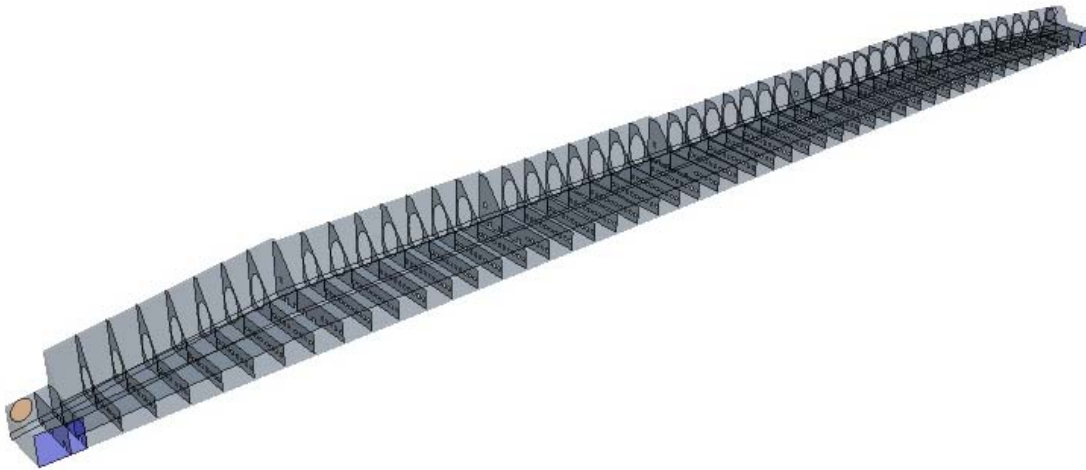


Figure 3.14: Computational Model of Double Bottom Ballast Trunk Structure

4. Experimental Investigation

The flow around the Ballast-Free Ship was tested experimentally in the towing tank of the MHL in July 2008. A different stock propeller was utilized in an attempt to validate the results obtained in January 2007 and also investigate the performance of a propeller with different characteristics (blade sections, pitch, and expanded area ratio). In addition to this, the resistance tests utilized updated MHL testing equipment that provided a more reliable prediction of the trunk flow on the vessel resistance. Finally, the vessel was also tested in the full load condition. The latter provided more accurate input in the Ballast-Free Ship powering investigation.

Plots of the International Towing Tank Conference (ITTC 1978) extrapolated ship resistance and effective power are shown in Figs. 4.1 and 4.2, respectively. Recall that effective power is the power equivalent of this total resistance obtained without a propeller so these show the same results. Even though there is some overlap in the error bands, there is a clear trend that the flow discharge increases the vessel's resistance. This trend was not obvious in results from the previous (January 2007) investigation. With discharge at Station 19, the resistance increase at the ballast speed of 15.5 knots is 2.44%. The corresponding increase for Station 17 is 4.61%. The form factor values were also computed for each case. The experimental results were found to be in relatively good agreement with the numerical results. The CFD results, however, over predict the form factor in all cases.

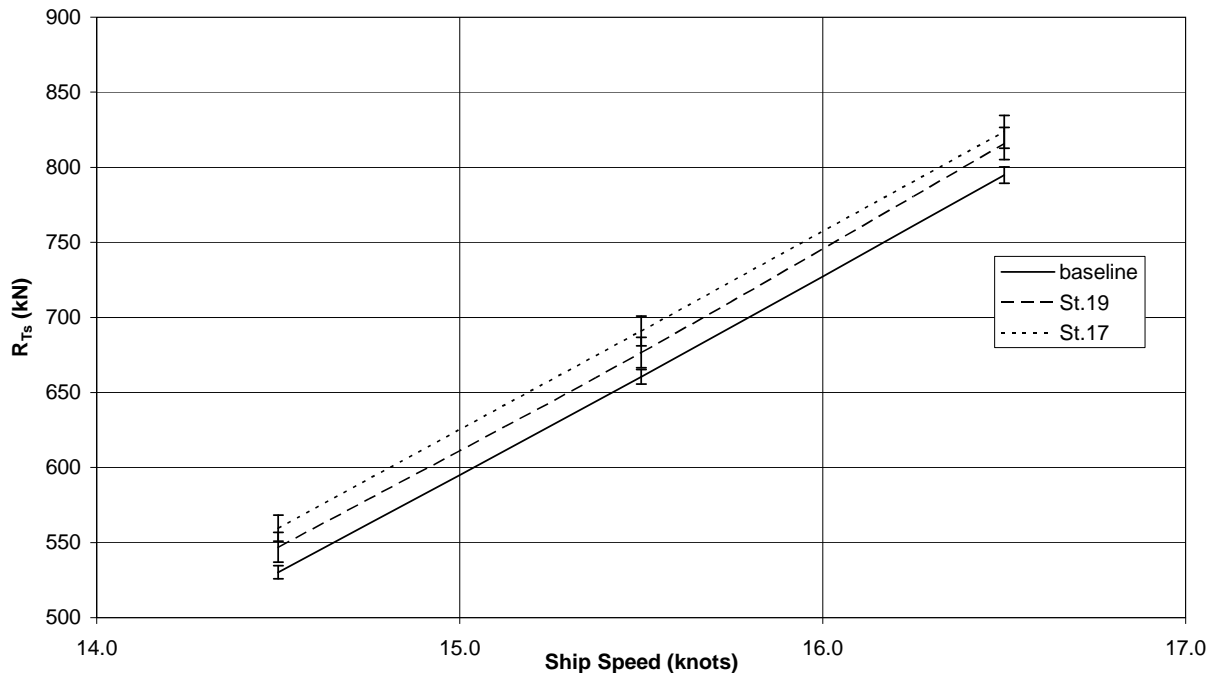


Figure 4.1: Ballast-Free Bulk Carrier Total Resistance

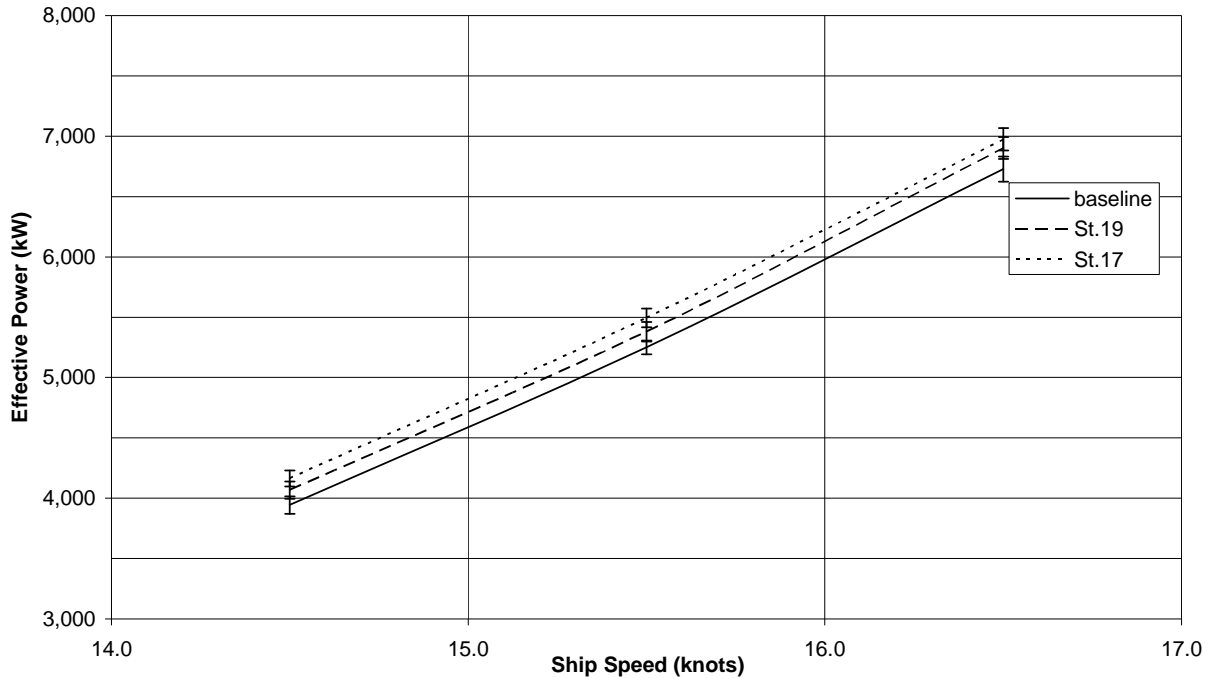


Figure 4.2: Ballast-Free Bulk Carrier Effective Power

Table 4.1: Form Factor Comparison

	CFD	Experiment
Baseline no trunk flow case	0.315	0.303
Discharge at St. 17 – 90min	0.306	0.283
Discharge at St. 19 – 90min	0.311	0.283

The model was also tested in the full load condition at the speed that corresponds to the full scale design speed of 14.5 knots. The extrapolated effective power was 7,114 hp, only slightly higher than the effective power in the ballast condition at 15.5 knots (7,042 hp). This validates the selection of the vessel speed in the ballast condition.

The characteristics of the No. 20 stock propeller used in the 2008 testing and the No. 23 stock propeller used in the 2007 testing are listed in Table 4.2.

Table 4.2: Characteristics of the MHL No. 20 and No. 23 Propellers

Characteristic	MHL No. 20	MHL No. 23
Number of blades, Z	4	4
Diameter (m)	0.159	0.158
Hub diameter (m)	0.032	0.031
Pitch-diameter ratio	0.80	1.08
Expanded area ratio	0.40	0.55

The propulsive performance was evaluated at the ballast speed. The discharge at Station 17 resulted in reduced powering requirements, compared to the baseline no trunk flow case, even though the reduction was significantly lower than that observed in the January 2007 testing for the discharge at this same location. Part of this change resulted from the higher, and more accurately determined total resistance change (4.6% in July 2008 vs. 2.7% in January 2007). These propulsion test results are summarized in Table 4.3.

Table 4.3: Propulsion Test Results - Ballast Condition at 15.5 knots

	Baseline No Trunk Flow Case	Discharge at St. 17 – 90min Exchange
Open water efficiency η_O	0.487	0.522
Wake fraction w	0.345	0.268
Thrust deduction t	0.287	0.167
Hull efficiency $\eta_H = (1 - t)/(1 - w)$	1.088	1.138
Relative rotative efficiency η_R	1.013	0.959
Behind propeller efficiency $\eta_P = \eta_O \eta_R$	0.493	0.501
Advance coefficient $J = V(1-w)/nD$	0.478	0.533
Propulsive efficiency $\eta_D = \eta_O \eta_H \eta_R$	0.536	0.570
Change in propulsive efficiency	base	+6.34%
Delivered power P_D (kW)	9,794	9,634
Change in required power	base	-1.63%

The total resistance R_T is related to the developed power P_D needed at the input to the propeller by the following:

$$P_D = R_T V / 1000 \eta_D \quad \text{kW} \quad (1)$$

where η_D is the product of the propeller open water efficiency η_O ; the relative rotative efficiency η_R , which corrects this to the behind the hull condition; and the hull efficiency η_H that is related to the wake fraction w and the thrust deduction t as shown in Table 4.3 (Parsons 2003). When the ballast trunk flow is introduced into the upper part of the propeller disk, all of these components change. With the added flow the wake fraction w changes downward as the flow becomes closer to vessel speed. With the acceleration of the stern flow, the propeller accelerates the flow less also reducing the thrust deduction t . The net effect is an important increase in the hull efficiency η_H . With a faster propeller inflow, the advance coefficient J operating point of the propeller increases as the propeller assumes a new operating point to supply the greater ship total resistance. This results in an increase in the open water efficiency η_O and behind the hull propeller efficiency η_P . With both η_H and η_P increasing, the overall propulsive efficiency η_D increases. This increase is large enough (6.34%) to overcome the total resistance increase (4.61%), i.e. $1.0461/1.0634 = 0.9837$, the 1.63% reduction in required power measured.

The fact that we didn't observe a similar reduction in powering requirements can be partially attributed to both the increase in measured resistance and the use of a different stock propeller.

The stock propeller utilized in July 2008 has blade sections with very low camber values; therefore, the propeller blades need to work at relatively high angles of attack to produce the required thrust and, thus, has lower open water efficiency. The propeller utilized in January 2007 (MHL #23) was able to demonstrate significantly better performance at the ballast condition in all cases (with and w/o discharge). The open water diagrams of the two propellers with the ship requirements in full load are shown in Fig. 4.3 for comparison.

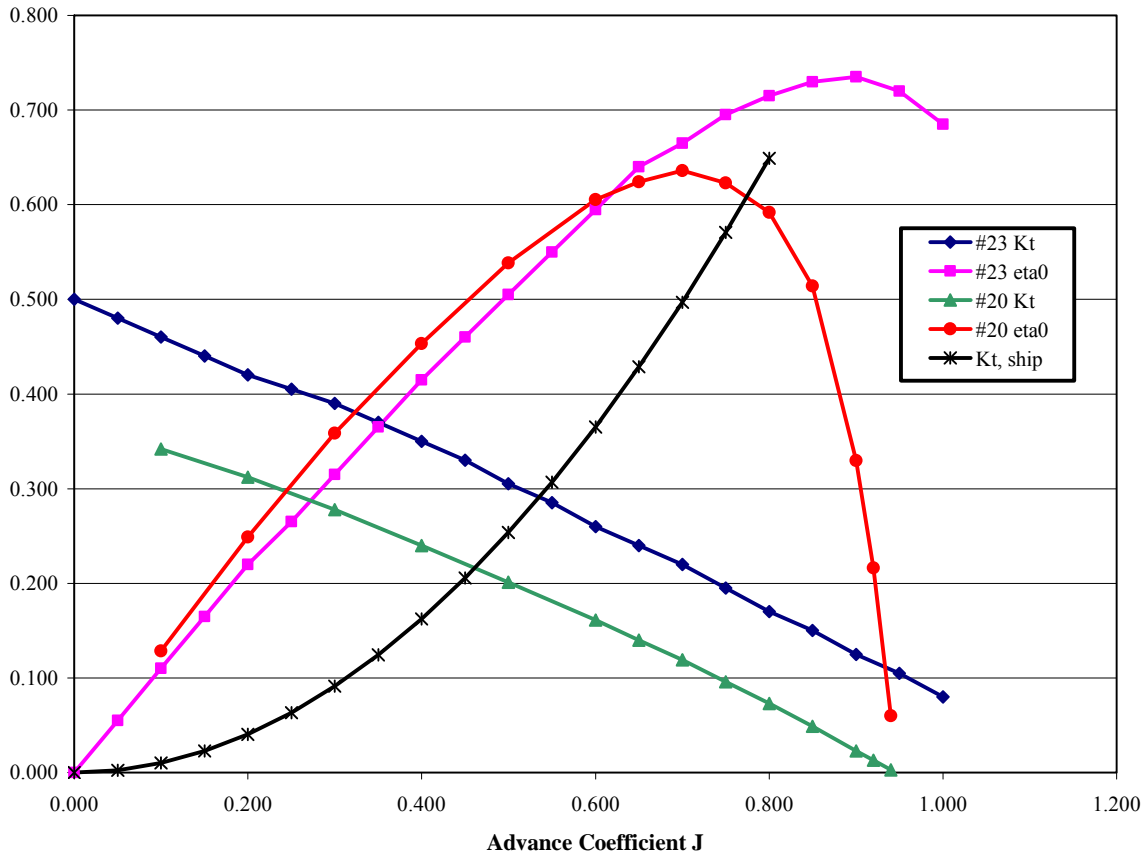


Figure 4.3: Stock Propeller Open Water Characteristics and Ship Thrust Requirement

There is also evidence that the Station 17 discharge experimental data that produced the large required power reduction (-7.3%) in the January 2007 experiments may have contained faulty data. When the direction of the change in w , t , J , η_O , and η_R (but not η_H and η_D) are compared between the baseline and the ballast flow cases found in the January 2007 tests with the discharge at Station 17 they are opposite to the direction of the changes found for the other tests as illustrated in Fig. 4.3. The direction of the changes found in the January 2007 tests with the discharge at Station 19 and the July 2008 tests with the discharge at Station 17 were consistent. This flawed data appears to be a third reason for very large required power reduction found in that January 2007 test with the discharge at Station 17. The results for this case as reported in Kotinis and Parsons 2007b appear to have been in error.

5. Potential Economic Impact of the Research Results

The economic impact of the Ballast-Free Ship concept on the capital and operating cost of a typical Seaway-sized bulk carrier was estimated in a manner similar to that used in the initial investigation of the concept (Kotinis et al. 2004). The results for the water discharge close to Station 17 are presented in Fig. 5.1. A realistic scenario was adopted for the economic analysis: a Handy-sized bulk carrier transporting grain from the upper Great Lakes (e.g. Duluth, Thunder Bay) to ports in Northern Europe and occasionally transporting steel into the Great Lakes. A North Atlantic voyage route between Rotterdam and Montreal, entering the Great Lakes through the St. Lawrence Seaway while in a ballast condition, is assumed.

A conservative assumption is that the 1.6% reduction in the required power of the Ballast Free bulk carrier will not be enough to permit a change in the main engine; thus, no propulsion machinery capital cost reduction was included. Foreign new construction, typical of Korea, was assumed for the calculation of the hull steel and other construction costs. The eliminated ballast water treatment system was assumed to consist of automatic backflush filtration as a primary treatment combined with UV irradiation for a secondary treatment. The estimated cost of this treatment equipment was based upon a study commissioned by the Great Lakes Ballast Technology Demonstration Project (Hurley et al. 2001).

The net savings in terms of the ΔRFR with the ballast trunk water discharge close to Station 17 is estimated to be about \$1.00 per tonne of cargo. This is relative to a typical 2008 grain freight rate to Europe of about \$100 per tonne and an annual cargo capacity for this vessel of 168,000 tonnes if it were only involved in this trade. These savings are relative to the use of filtration primary and UV secondary ballast water treatment when ballast water exchange is no longer permitted in the future.

Economics Summary			
<i>Vessel data and trip scenario</i>	<i>Typical bulk carrier</i>	<i>Ballast-free bulk carrier</i>	<i>Comments</i>
Round-trip distance (nautical miles)		6,280	Great Lakes via Seaway and Montreal (CAN) to Rotterdam (NL)
Service speed (kts)		15.0	Typical data for an ocean-going Handymax bulk carrier transporting grain cargo from the Great Lakes (Duluth, Thunder Bay) to ports in Northern Europe and occasionally transporting steel into the Great Lakes.
Speed in ballast condition (kts)		15.5	
Proportion of miles in ballast (%)		35	
Average Seaway loaded cargo / maximum cargo (%)		75	
Load factor (%)		48.8	
Days of navigation through the Great Lakes		8	Passage up through the Great Lakes towards the western end
Port days per round trip		14	Includes loading/unloading time, bunkering time, and time waiting for berth
Round trips per annum		7	
Maximum payload (metric tons)		32,000	
Cargo carried per annum (metric tons)		168,000	
Engine nominal MCR (kW)		8,580	Data for the MAN B&W 6S50MC two-stroke engine
Block coefficient	0.835	0.841	Compensate for increased hull steel weight and lost buoyancy at plena
Hull steel weight (metric tons)	5,550	5,770	
Hull steel cost (\$)	3,885,000	4,039,000	Assuming a Korean steel price of \$700/metric ton
Continuous service rating in ballast condition (kW)	7,700	7,575	Includes 15% sea margin and effect of change in C _B value
Continuous service rating in Seaway draft condition (kW)	7,700	7,590	Includes 15% sea margin and effect of inlet/outlet hull openings and change in C _B value
Specific fuel consumption (g/(kW*hr))	168.7	168.1	Data for the MAN B&W 6S50MC engine, ISO ambient conditions
Annual heavy fuel cost (\$)	2,101,000	2,062,000	Fuel price (IFO380) of \$558.30/metric ton (9/23/2008), transatlantic part of trip only
Changes in capital cost with Discharge at Sta. 17			
Additional hull steel cost (\$)		154,000	
Sluice gates cost (\$)		260,000	Acquisition cost plus labor for 52 450x600 mm sluice gates (@ \$5,000 each)
Elimination of ballast tank valves (\$)		-14,000	14 @ 1,000 each
Reduction in ballast piping cost (\$)		-314,000	Removal of main ballast headers (material plus labor)
Reduction in welding cost (\$)		-9,500	Reduced welding at the bottom of solid floors (material plus labor)
Additional ballast piping cost (\$)		79,000	Addition of ballast piping for F.P. tank (material plus labor)
Additional welding cost (\$)		2,600	Additional welding due to raise of inner bottom (material plus labor)
Elimination of ballast water treatment system (\$)		-634,500	Assuming automatic backflush filtration combined with UV irradiation
Net capital cost change (\$)		-476,400	
Changes in operating cost with Discharge at Sta. 17			
Change in heavy fuel oil cost (\$)		-39,000	
Elimination of ballast water treatment system operating cost (\$)		-77,920	Fuel price (MDO) of \$871.50/metric ton (Rotterdam, 9/23/2008), (www.bunkerworld.com)
Net operating cost change per annum (\$)		-116,920	
Capital recovery factor		0.1175	i = 10%, n = 20 years
Change in required freight rate (\$/metric ton)		-1.03	savings

Figure 5.1: Order of Magnitude Economics Comparing a Typical Bulk Carrier with Filtration and UV Treatment with Ballast-Free Bulk Carrier

6. Dissemination of Study Results

During this past year, the project worked with University of Michigan New Services (Jim Erickson) to prepare a 5 min video and news release describing the Ballast-Free Ship concept and the testing sponsored by GLMRI. This was featured on the University website and a parallel article has appeared in *The University RECORD*, the in-house UM newspaper. The video has also been included on YouTube. The news spot has been picked up or utilized for articles by numerous organizations including the following:

UPI
Washington Post
WWJ radio in Detroit
The Naval Architect of RINA
Mechanical Engineer of ASME
Technish Weekblad in Denmark
Surveyor, to be published by the American Bureau of Shipping
Discover magazine
Polish *Newsweek* magazine
Estuary of the San Francisco Estuary Project
Conservation
Business Week
Prism of the American Association for Engineering Education
Frontiers of Ecology
Ingenioren, Denmark
Scandinavian Shipping Gazette
Ballast Exchange Newsletter
Inventique

Parsons was interviewed for a spot that appeared on National Public Radio's *Environmental Report*. A short invited article authored by Parsons and Kotinis appeared in the May environmental issue of *Maritime Reporter*. A short invited article by Parsons appeared in the 2008 *Yearbook of Maritime Technology* published by the *Scandinavian Shipping Gazette*. A short article by Parsons and Kotinis has also been submitted for inclusion in a fall 2008 issue of *Great Lakes/Seaway Review*. The support of GLMRI has been mentioned whenever feasible.

Parsons has been contacted informally by three parties (two U.S. and one Korean) concerning opportunities and interest in participating in the commercialization of the Ballast-Free Ship concept.

The following publications during the past year were related to this funded research:

- Kotinis, M. and Parsons, M. G., "Hydrodynamic Optimization of the Ballast-Free Ship Concept" *Transactions SNAME*, **115**, 2007. This paper received the ABS/Captain Joseph H. Linnard Prize for the Best Paper presented before the society in 2007

- Parsons, M. G. and Kotinis, M., “Recent Testing Indicates the Ballast-Free Ship Concept can also Provide Fuel Savings,” *Maritime Reporter*, May 2008.
- Parsons, M. G., “An alternative solution to ballast water treatment: the Ballast-Free Ship concept,” *2008 Yearbook of Maritime Technology, Scandinavian Shipping Gazette*, 2008.
- Parsons, M. G. and Kotinis, M., “Ballast-Free Ship Concept Testing Shows a Potential Fuel Savings,” to appear in *Great Lakes/Seaway Review*, fall 2008.

The following presentations during the past year were related to this funded research:

- Kotinis, M. and Parsons, M. G., “Hydrodynamic Optimization of the Ballast-Free Ship Concept” to be presented at the Society of Naval Architects and Marine Engineers Annual Meeting, Ft. Lauderdale, FL, Nov. 2007.
- Parsons attended and presented a summary of this project at the GLMRI Affiliates Meeting, September 23, 2008, in Superior, WI.
- Kotinis and Parsons will present a paper on the results of the project at the meeting of the Great Lakes and Great Rivers of SNAME in Ann Arbor, MI, on November 13, 2008.

The results of the funded research were reviewed in the following class:

- It is understood that the results of this investigation were reviewed in the graduate class NA570 Advanced Marine Design at the University of Michigan in the Winter Semester 2008.

7. References

- Ballast Water News 2004 "The Ballast-Free Ship - Fact or Fancy?" *Ballast Water News*, Global Ballast Water Management Program, IMO, **17**, April-June.
- Hurley, W. L. JR., Schilling, S. S. JR. and Mackey, T. P. 2001 "Contract Designs for Ballast Water Treatment Systems on Containership *R. J. Pfeiffer* and Tanker *Polar Endeavor*," SNAME/ ASNE Marine Environmental Engineering Technical Symposium, Arlington, VA, May 31-June 1 (CD).
- IMO 2004 "International Convention for the Control and Management of Ships' Ballast Water & Sediments," Diplomatic Conference, February, London.
- ITTC 1978 "15th International Towing Tank Conference, 3-10 September 1978, The Hague, The Netherlands", Netherlands Ship Model Basin, Wageningen.
- Kotinis, M., Parsons, M. G., Lamb, T. and Sirviente, A. 2004 "Development and Investigation of the Ballast-Free Ship Concept," *Transactions SNAME*, **112**, pp. 206-240.
- Kotinis, M. 2005 "Development and Investigation of the Ballast-Free Ship Concept," Ph.D. Dissertation, University of Michigan, Department of Naval Architecture and Marine Engineering.
- Kotinis, M. and Parsons, M. G. 2007a "Numerical Investigation of the Flow at the Stern of a Ballast-Free Bulk Carrier Model" *Proceedings of the 9th Int. Conference in Numerical Ship Hydrodynamics*, Aug.
- Kotinis, M. and Parsons, M. G. 2007b "Hydrodynamic Optimization of the Ballast-Free Ship Concept" *Transactions SNAME*, **115**, pp. 50-67.
- Parsons, M. G. 2003 "Parametric Design," Ch. 11 in Lamb, T. (ed.), *Ship Design and Construction*, SNAME, Jersey City, NJ.
- Parsons, M. G. and Kotinis, M. 2006 "Seaway-Sized Bulk Carrier Model for Hydrodynamic Optimization of Ballast-Free Ship Design," GLMRI Annual Report, October 2.
- Parsons, M. G. and Kotinis, M. 2007 "Hydrodynamic Optimization Testing of Ballast-Free Ship Design," GLMRI Annual Report, October 30.
- U. S. Patent #6,694,908 2004 "Ballast Free Ship System," U. S. Patent and Trademark Office, Washington, DC.